Radio Recombination Lines from Starbursts: NGC 3256, NGC 4945 and the Circinus Galaxy

A. L. Roy*, W. M. Goss†, Niruj R. Mohan**, T. Oosterloo‡ and K.R. Anantharamaiah§

*Max-Planck-Institut für Radioastronomie, Auf dem Hügel 69, 53121 Bonn, Germany
†NRAO, PO Box O, Socorro, NM 87801, USA
**Raman Research Institute, CV Raman Ave, Sadashivanagar, Bangalore 560080, India
‡ASTRON, PO Box 2, 7990 AA, Dwingeloo, The Netherlands
§Raman Research Institute, CV Raman Ave, Sadashivanagar, Bangalore 560080, India; (deceased)

Abstract.
A renewed attempt to detect radio recombination lines from external galaxies has resulted in the measurement of lines from several bright starburst galaxies. The lines are produced by hydrogen ionized by young, high-mass stars and are diagnostic of the conditions and gas dynamics in the starburst regions without problems of dust obscuration. We present here detections of the lines H91α and H92α near 8.6 GHz from the starburst nuclei in NGC 3256, NGC 4945, and the Circinus galaxy using the ATCA and VLA. Modelling the line emitting region as a collection of H II regions, we derive the required number of H II regions, their temperature, density, and distribution.

INTRODUCTION

Radio recombination lines (RRLs) from nuclear starbursts pass unattenuated through dust and so their strength tells about conditions in the starburst without uncertainty caused by unknown extinction that troubles optical and near-infrared studies.

The potential for detecting extragalactic RRLs was first pointed out by [1] and shortly thereafter RRLs were detected from the starbursts in M 82 and NGC 253 ([2], [3]). These two galaxies have since been studied at many frequencies, yielding the physical state and kinematics in the nuclear regions (e.g. [4], [5]).

Then came a period of surveys that yieled no further detections ([6], [7], [8]). A renewed effort during the early 1990s using the Very Large Array (VLA) with improved sensitivity detected RRLs near 8.6 GHz from several bright starburst galaxies at a level 10$\times$ weaker than the first two detections. These new detections are NGC 660, NGC 1365, NGC 2146, NGC 3628, NGC 3690, NGC 5253, M 83, IC 694, Arp 220, Henize 2-10 ([9], [10], [11], [12]), NGC 1808 ([13]), and NGC 4945 at mm wavelengths ([14]).

We present here three new detections: NGC 3256, NGC 4945 and the Circinus galaxy.

NEW ATCA AND VLA OBSERVATIONS

We selected five nearby (< 40 Mpc), infra-red luminous ($L_{\rm FIR} > 10^{10}\ L_{\odot}$), dusty ($L_{\rm FIR}/L_{\rm optical} > 2$) bright ($S_{100\mu{\rm m}} > 10$ Jy) starburst galaxies (NGC 3256, NGC 4945,

NGC 6221, NGC 7552 and the Circinus Galaxy) to survey for RRL emission. We also selected two nearby bright type 2 Seyfert galaxies (IC 5063 and Fairall 49) to see whether the ionized gas in the narrow-line region might also be detected.

We observed each galaxy for 10 h to 30 h with the ATCA [1] and made a confirmation observation of NGC 3256 with the VLA [2]. With the ATCA we observed simultaneously the lines H91α and H92α near 8.6 GHz. With the VLA we observed H92α.

A bandpass calibrator was observed every few hours and phase corrections obtained from self calibration of the continuum source were applied to the spectral line data. We subtracted the continuum emission using a linear fit to each baseline spectrum using with UVLSF ([15]). The final images were made using natural or robust weighting to achieve near-maximum possible signal-to-noise ratio.

We did not detect H91α + H92α emission from NGC 6221, NGC 7552, IC 5063 and Fairall 49 after 10 h integrations reaching rms of 0.35 mJy beam per 1 MHz channel.

DETECTION OF NGC 3256

NGC 3256 is a pair of colliding disk galaxies 37 Mpc distant (for $H_0 = 75$ km s^{-1} Mpc^{-1}) that are merging and display spectacular tidal tails (e.g. [16]). The FIR luminosity is $1.9 \times 10^{11} L_\odot$ following the method of [17], and the molecular gas mass, from CO emission, is large ($3 \times 10^{10} M_\odot$, [18]). The Brγ and [Fe II] luminosities imply a total star formation rate of 3.9 $M_\odot$ yr^{-1}. VLA observations at 6 cm with 4" resolution by [19] show emission over 30" and arms of diffuse emission extending out towards the giant tidal arms seen in H I ([20]). At higher resolution (2"), [21] resolve the nucleus into two equal components; the nuclei of the progenitor galaxies are both undergoing starbursts.

Our ATCA discovery observation is shown in Fig 1. Integration time was 24.2 h with 1 MHz (35 km s^{-1}) channels. The 8.4 h VLA follow-up observation with sensitivity of 0.081 mJy beam^{-1} channel^{-1} yielded an essentially similar result and is shown in [22].

We used the observed line strength (1.0 mJy), line width (160 km s^{-1}), size of the line-emitting region (630 pc), continuum emission (116 mJy) and spectral index (-0.7) to constrain conditions in the ionized gas. We considered a simple model consisting of a collection of spherical H II regions, all with the same diameter, electron temperature, T_e, electron density, n_e, in a volume of uniform synchrotron emission, following [9]. Models with 10 to 300 H II regions, all with $T_e \sim 5000$ K, $n_e \sim (10^3$ to $10^4)$ cm^{-3} and size of (5 to 600) pc produced good matches to the line and continuum emission.

The inferred mass of ionized gas is 4×10^4 $M_\odot$ to 2×10^5 $M_\odot$, depending on the model conditions, which requires a Lyman continuum flux of 2×10^{52} s^{-1} to 6×10^{53} s^{-1} to maintain the ionization. This flux is equivalent to the Lyman continuum output of 600 to 17000 stars of type O5, which infers a star-formation rate of (0.5 to 14) $M_\odot$ yr^{-1} when averaged over the lifetime of OB stars.

---

[1] The Australia Telescope Compact Array is part of the Australia Telescope, which is funded by the Commonwealth of Australia for operation as a National Facility managed by CSIRO.

[2] The National Radio Astronomy Observatory is a facility of the National Science Foundation operated under cooperative agreement by Associated Universities, Inc.

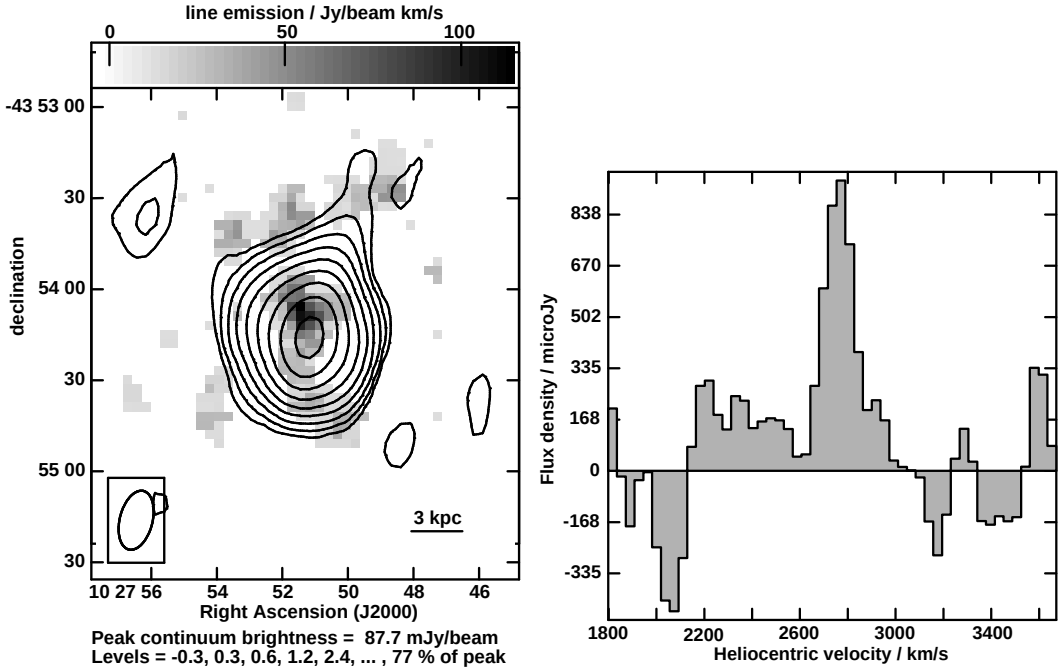

FIGURE 1. Left: ATCA 8.4 GHz continuum image of NGC 3256 observed 1994 Oct + 1995 Aug (contours), superimposed on the grey scale zeroth-moment image showing H91α + H92α line emission. Beamsize is $16.4'' \times 9.6''$. The offset between the line and continuum peaks is perhaps significant as it was seen also in the VLA observation. Right: ATCA H91α + H92α line profile integrated over the line-emitting region in NGC 3256, observed 1994 Oct + 1995 Aug. RMS noise is 0.14 mJy beam^{-1} channel^{-1}.

DETECTION OF NGC 4945

NGC 4945 is a nearby (3.9 Mpc[23]) edge-on spiral galaxy containing an obscured nuclear starburst and is the second-brightest Seyfert 2 galaxy in the X-ray sky at 100 keV [24]. Its nucleus hosts water masers with up to 10 Jy [25].

Our ATCA discovery observation is shown in Figs 2 and 3. Integration time was 22.7 h with 35 km s^{-1} channel^{-1} and sensitivity of 0.16 mJy beam^{-1} channel^{-1}.

We used the integrated line strength (11.0 mJy), line width (280 km s^{-1}), size of the line-emitting region (70 pc), continuum emission (1439 mJy), and spectral index (-0.75) to constrain conditions in the ionized gas. Using the collection of H II regions model, models with 10 to 300 H II regions, all with $T_{\rm e} \sim 5000$ K, $n_{\rm e} \sim 10^3$ cm^{-3} to 10^4 cm^{-3} and size of (2 to 100) pc produced good matches to the line and continuum emission.

The inferred mass of ionized gas is $2 \times 10^5\ M_\odot$ to $6 \times 10^5\ M_\odot$, depending on the model conditions, which requires a Lyman continuum flux of 6×10^{52} s^{-1} to 3×10^{53} s^{-1} to maintain the ionization. This flux is equivalent to the Lyman continuum output of 2000 to 10000 stars of type O5, which infers a star-formation rate of (2 to 8) $M_\odot$ yr^{-1} when averaged over the lifetime of OB stars.

We fitted to the rotation curve a simple model consisting of a set of rings which were coplanar and edge-on. The brightness of each ring was determined by deprojecting the observed zeroth-moment image to derive the radial distribution of the line intensity. The

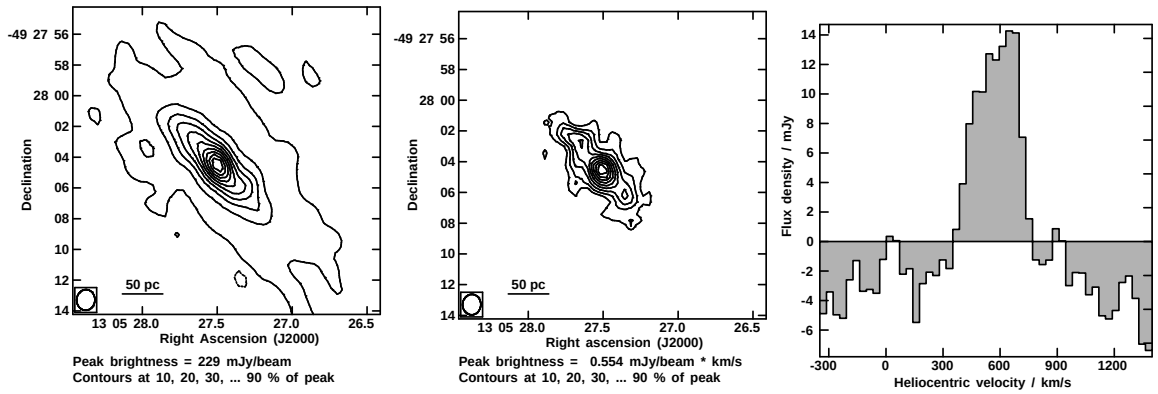

FIGURE 2. Left: ATCA 8.3 GHz + 8.6 GHz continuum image with uniform weight of NGC 4945 observed for 22.7 h on 1993 Jul 25 + 1994 Sep 22 + 1994 Oct 04 (contours). Middle: ATCA zeroth-moment image of H91α + H92α emission. Beamsize is $1.4'' \times 1.2''$. Right: ATCA H91α + H92α line profile integrated over line-emitting region in the zeroth-moment image. RMS noise is 0.16 mJy beam^{-1} channel^{-1}.

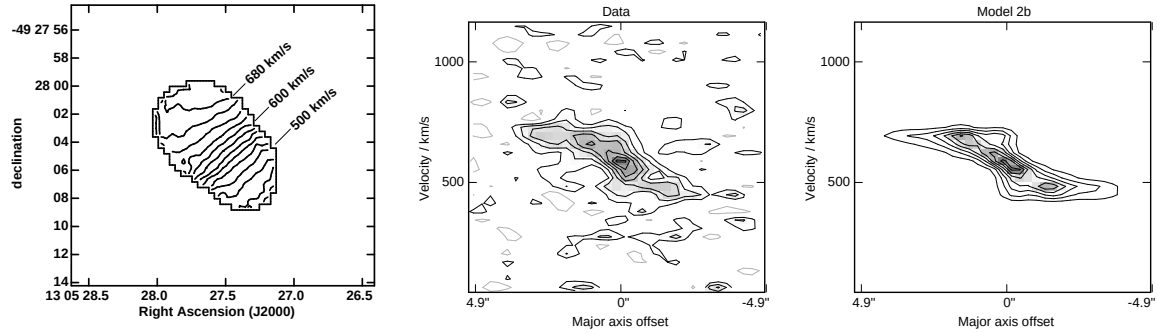

FIGURE 3. Left: ATCA first-moment image of H91α + H92α emission showing rotation. Beamsize is $1.4'' \times 1.2''$. Middle: H91α + H92α rotation curve along the major axis of the line-emitting region. Right: Rotation curve from the best-fit dynamical model

radial distribution showed a central peak and a ring of emission 2.5" (50 pc) from the nucleus.

We refined the model iteratively, varying the systemic velocity, rotation velocity, and velocity dispersion until we achieved a reasonably close match to the data, and found no reason to depart from a simple flat rotation curve. We refined the radial profile of line emission strength, increasing the central peak at the systemic velocity to 25 times the brightness of the more extended emission. The final model had a flat rotation curve with $v_{\rm systemic} = 581$ km s^{-1}, $v_{\rm rotation}$ = 120 km s^{-1}, and $v_{\rm dispersion}$ = 15 km s^{-1}. We did not need to invoke a bar or radial motion, though the data do not strongly exclude either.

The rotation velocity of 120 km s^{-1} within the central 1" (19 pc) radius infers an enclosed mass of $3 \times 10^7 M_\odot$. The water masers ([26]) infer an enclosed mass of $1 \times 10^6 M_\odot$ within 0.3 pc radius, and so most of the $3 \times 10^7 M_\odot$ is extended between 0.3 pc and 19 pc radius of the nucleus. The average surface density within the central 19 pc is 25000 $M_\odot$ pc^{-2}, which exceeds the threshold gas surface density for star-formation of

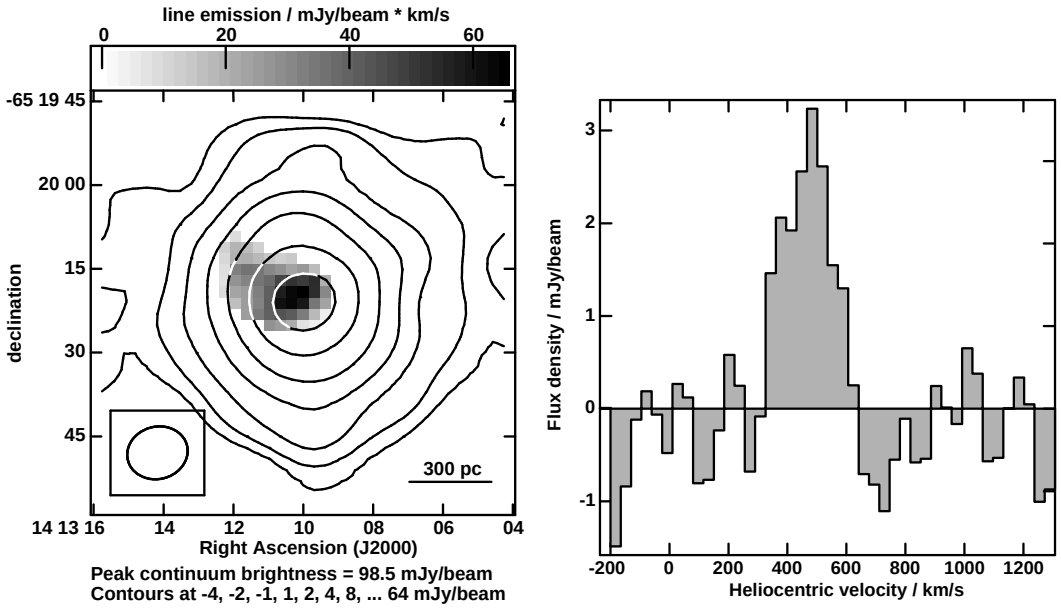

FIGURE 4. Left: ATCA 8.4 GHz continuum image of the Circinus Galaxy observed for 37 h on 1993 Jul + 1994 Oct + 1994 Nov (contours), superimposed on the grey scale zeroth-moment image showing H91α + H92α line emission. Beamsize is $11.0'' \times 9.4''$, rms noise is 0.12 mJy beam^{-1} channel^{-1}. Right: ATCA H91α + H92α line profile integrated over the line-emitting region in the Circinus Galaxy.

(3 to 10) $M_\odot$ pc^{-2} ([27]) by four orders of magnitude.

The 50 pc ring might be a Lindblad resonance, which would infer a bar. The bright peak in the line emission at the nucleus might be recombination-line maser emission occuring along the line of sight towards the nucleus. In that direction, the gas velocity is transverse to the line of sight and so gas at all distances share a common velocity, which maxizes the path length over which RRL maser amplification can occur.

DETECTION OF THE CIRCINUS GALAXY

The Circinus Galaxy, at a distance of 4.2 Mpc[28], is situated behind the Galaxy and evaded discovery until relatively recently [28]. It hosts a nuclear starburst and an obscured Seyfert nucleus, and is a water megamaser source [29].

Our ATCA observations discovered RRL emission, which is shown in Fig 4.

We used the observed line strength (3.2 mJy), line width (280 km s^{-1}), size of the line-emitting region (250 pc), continuum emission (225 mJy), and spectral index (-0.65) to constrain conditions in the ionized gas. The collection of H II regions model with 15 to 10000 H II regions, all with $T_e \sim 5000$ K, $n_e \sim (500 \text{ to } 5 \times 10^4)$ cm^{-3} and size of (3 to 50) pc produced good matches to the line and continuum emission.

The inferred mass of ionized gas is $3 \times 10^3\ M_\odot$ to $1 \times 10^6\ M_\odot$, depending on the model conditions, which requires a Lyman continuum flux of 1×10^{52} s^{-1} to 3×10^{53} s^{-1} to maintain the ionization. This flux is equivalent to the Lyman continuum output of 300

to 2000 stars of type O5, which infers a star-formation rate of (0.2 to 2) $M_\odot$ yr^{-1} when averaged over the lifetime of OB stars.

CONCLUSION

Seven galaxies were observed with the ATCA and one also with the VLA. These yielded a spectacular detection of NGC 4945, and good detections of NGC 3256 and the Circinus Galaxy. Four other galaxies were not detected. From the detections we derived physical conditions and kinematics in the ionized gas in the nuclear starbursts.

Future observations at high frequencies where RRLs are stronger and resolution is higher will provide measurements of multiple transitions to provide tighter constraints on the gas conditions, and the upcoming sensitivity improvements coming with the EVLA, ALMA and SKA will make tremendous impact on this work.

REFERENCES

1. Shaver, P. A., *A&A*, **68**, 97 (1978).
2. Shaver, P. A., Churchwell, E., and Rots, A. H., *A&A*, **55**, 435 (1977).
3. Seaquist, E. R., and Bell, M. B., *A&A*, **60**, L1 (1977).
4. Anantharamaiah, K. R., and Goss, W. M., "New Results from H92 alpha Recombination Line Observations of NGC 253," in *Revista Mexicana de Astronomia y Astrofisica Conference Series*, 1997, p. 58.
5. Rodriguez-Rico, C. A., Goss, W. M., Viallefond, F., and Zhao, J.-H., *American Astronomical Society Meeting*, **204**, 62.24 (2004).
6. Churchwell, E., and Shaver, P. A., *A&A*, **77**, 316 (1979).
7. Bell, M. B., and Seaquist, E. R., *ApJ*, **223**, 378 (1978).
8. Bell, M. B., Seaquist, E. R., Mebold, U., Reif, K., and Shaver, P., *A&A*, **130**, 1 (1984).
9. Anantharamaiah, K. R., Zhao, J., Goss, W. M., and Viallefond, F., *ApJ*, **419**, 585 (1993).
10. Zhao, J., Anantharamaiah, K. R., Goss, W. M., and Viallefond, F., *ApJ*, **472**, 54 (1996).
11. Phookun, B., Anantharamaiah, K. R., and Goss, W. M., *MNRAS*, **295**, 156 (1998).
12. Mohan, N. R., Anantharamaiah, K. R., and Goss, W. M., *ApJ*, **557**, 659 (2001).
13. Mohan, N. R., *PhD Thesis* (2002).
14. Viallefond, F., *Private communication* (2004).
15. Cornwell, T. J., Uson, J. M., and Haddad, N., *A&A*, **258**, 583 (1992).
16. Schweizer, F., *Science*, **231**, 227 (1986).
17. Helou, G., Soifer, B. T., and Rowan-Robinson, M., *ApJ*, **298**, L7 (1985).
18. Sargent, A. I., Sanders, D. B., and Phillips, T. G., *ApJ*, **346**, L9 (1989).
19. Smith, E. P., and Kassim, N. E., *AJ*, **105**, 46 (1993).
20. English, J., Norris, R. P., Freeman, K. C., and Booth, R. S., *AJ*, **125**, 1134 (2003).
21. Norris, R. P., and Forbes, D. A., *ApJ*, **446**, 594 (1995).
22. Roy, A. L., Goss, W. M., Mohan, N. R., and Anantharamaiah, K. R., *A&A*, *submitted* (2004).
23. Bergman, P., Aalto, S., Black, J. H., and Rydbeck, G., *A&A*, **265**, 403 (1992).
24. Done, C., Madejski, G. M., and Smith, D. A., *ApJ*, **463**, L63 (1996).
25. Whiteoak, J. B., and Gardner, F. F., *MNRAS*, **222**, 513 (1986).
26. Greenhill, L. J., Moran, J. M., and Herrnstein, J. R., *ApJ*, **481**, L23 (1997).
27. Kennicutt, R. C., *ApJ*, **344**, 685 (1989).
28. Freeman, K. C., Karlsson, B., Lynga, G., Burrell, J. F., van Woerden, H., Goss, W. M., and Mebold, U., *A&A*, **55**, 445 (1977).
29. Gardner, F. F., and Whiteoak, J. B., *MNRAS*, **201**, 13P (1982).